RSC Advances

RSC Advances

www.rsc.org/advances

ROYAL SOCIETY OF CHEMISTRY

www.rsc.org/advances

pH-Degradable and Thermoresponsive Water-Soluble Core Cross-Linked Polymeric Nanoparticles as Potential Drug Delivery Vehicle for Doxorubicin

Rakesh Banerjee [†], Sheetal Parida [‡], Chiranjit Maiti [†], Mahitosh Mandal [‡,] and Dibakar

Dhara [†,]*

[†] Department of Chemistry

[‡] School of Medical Science and Technology

Indian Institute of Technology Kharagpur

West Bengal 721302 India

AUTHOR INFORMATION

*Corresponding Author:

Email: dibakar@chem.iitkgp.ernet.in, dibakar@live.in

Ph no: +91-3222-282326; Fax: +91-3222-282252

ABSTRACT

Controlled and efficient delivery of therapeutics to tumor cells is one of the key issues in cancer therapy. In the present work, a new class of water soluble polymeric core cross-linked nanoparticles (CLPNs) possessing acid degradable core and thermoresponsive shell was synthesized for pH-triggered delivery of drug to cancerous cell. The diol groups of poly(ethylene glycol)-*b*-poly(N-isopropylacrylamide)-*b*-poly(glycidyl methacrylate) diol triblock copolymer were utilized to form the core cross-linked polymeric nanoparticles through arm-first method by reaction with aldehyde functionalized cross-linkers through formation of acetal linkages. The encapsulation efficiency as well as the release properties of these CLPNs was investigated using doxorubicin (DOX), a known anticancer drug. The release was found to be preferable at the desired lysosomal pH (~5.0) of the cancer cells and below the LCST (~32 °C) of poly(N-isopropylacrylamide) (PNIPA). The cytotoxicities of the precursor polymer as well as the CLPNs were tested on the growth NIH/3T3, normal mouse fibroblast cells, and were found to be nontoxic. The anticancer activity of the DOX loaded CLPN was confirmed using cervical cancer cell lines HeLa and SiHa by MTT assay, morphological studies and flow cytometry. These studies revealed an increased accumulation of the drug around the nucleus when treated with DOX-loaded CLPN as compared to free DOX along with significant reduction in IC50 of both the cell lines. Thus, these CLPNs are potentially useful for controlled drug delivery in case of advanced chemotherapeutic applications.

INTRODUCTION

Doxorubicin (DOX) is a one of the most potent and commonly used chemotherapeutic drug used as a monodrug treatment against different forms of cancers including hematological malignancies, solid tumors and soft tissue carcinoma.[1] It is also used as a combination therapy in many other chemotherapeutic regimens. However, it is also known to be associated with various serious side effects e.g. hair loss, myelosuppression, nausea and vomiting, oral mucositis, oesophagitis, diarrhoea; the most dangerous ones being heart damage and liver dysfunction.[2] Owing to its high potency as well as severe side effects, many targeted delivery systems have been designed in the past decade that include polymer based drug delivery systems.[3-6] PEGylated liposome encapsulated doxorubicin, commercially available as Doxil, has proved to be a highly effective treatment against recurrent ovarian cancer which has failed platinum based chemotherapy and AIDS related Kaposi sarcoma. We have also reported a polymer tethered magnetic nanoparticle system as a potent targeted delivery system for DOX.[8]

In recent times, polymeric nanostructures have also shown exciting results in the field of controlled and targeted delivery of anticancer drugs like DOX. Stimuli-responsive polymeric nanostructures with dynamic covalent bonds (DCBs) have become particularly important for their fascinating target specific controlled delivery properties.[9] Among these, polymeric nanocarriers with acid cleavable DCBs like imine, hydrazone, and ester have shown potential applicability in biological system due to their release capability under desired lysosomal pH (~5.0) of the cancer cells.[10-12] Furthermore pH degradable cross-linked polymer nanostructures are advantageous as they retain their structural integrity even in dilute solutions unlike uncross-linked nanostructures that are likely to disintegrate on dilution when injected into the body, thereby releasing the payload in unwanted places. Hence, synthesis of core and shell cross-linked nanostructures like micelles, nanoparticles and nanogels with thermoresponsive and degradable

cores have been subjects of interest owing to their numerous applications in the field of delivery of drugs and biomolecules.[13-17]

The two main approaches towards synthesis of cross-linked nanostructures that have been explored are - shell cross-linking as reported by Wooley et al.,[18-19] Armes et al.,[20-21] and McCormick et al.,[22-23] and core cross-linking as reported by Wiltshire and Qiao,[24-25] Sumerlin et al.,[26-27] and Fulton et al.[10,28] Several approaches have been explored for the development of degradable and thermoresponsive cores using poly(N-isopropylacrylamide) (PNIPA) or poly(methoxydiethylene glycol methacrylate) as thermoresponsive polymers, and acid- or photo-degradable and reductive disulphide breakable molecules as cross-linkers. McCormick et al.[22,29] and Fulton et al.[30-31] have synthesized a wide range of thermoresponsive and pH-degradable shell and core cross-linked polymer assemblies respectively using thermoresponsive PNIPA and acid cleavable imine bond. Core cross-linked micelles or nanogels, with labile core that are sensitive to weakly acidic and reductive environment, are promising developments that have found significant interest in the field of chemotherapy.[32-38] However, it is very important to find newer method(s) of cross-linking, especially the ones that enable pH-triggered de-crosslinking/degradation, thereby releasing the entrapped drug molecules in a pH-responsive manner.

In this work, we report the use of acetal linkage to form cross-linking which undergo de-crosslinking at lysosomal pH of cancer cells (~5.0). A simple approach for the synthesis of core cross-linked polymeric nanoparticles (CLPNs) through diol-aldehyde acetal formation between a diol functionalized triblock copolymer and aldehyde functionalized cross-linker was established. We have further investigated the pH triggered disassembly of the cross-linked nanoparticles, in order to check their effectiveness in the field of controlled release of drug molecules. Doxorubicin (DOX) was encapsulated in the core of the nanoparticles and their drug release

behaviors at various pH values and temperatures were evaluated. The cytotoxicities of the free polymer and CLPNs on the growth of normal mouse fibroblasts, NIH/3T3, as well as cervical cancer cells, HeLa and SiHa were tested, and the anticancer activity of the DOX loaded CLPN was investigated using HeLa and SiHa cervical cancer cell lines.
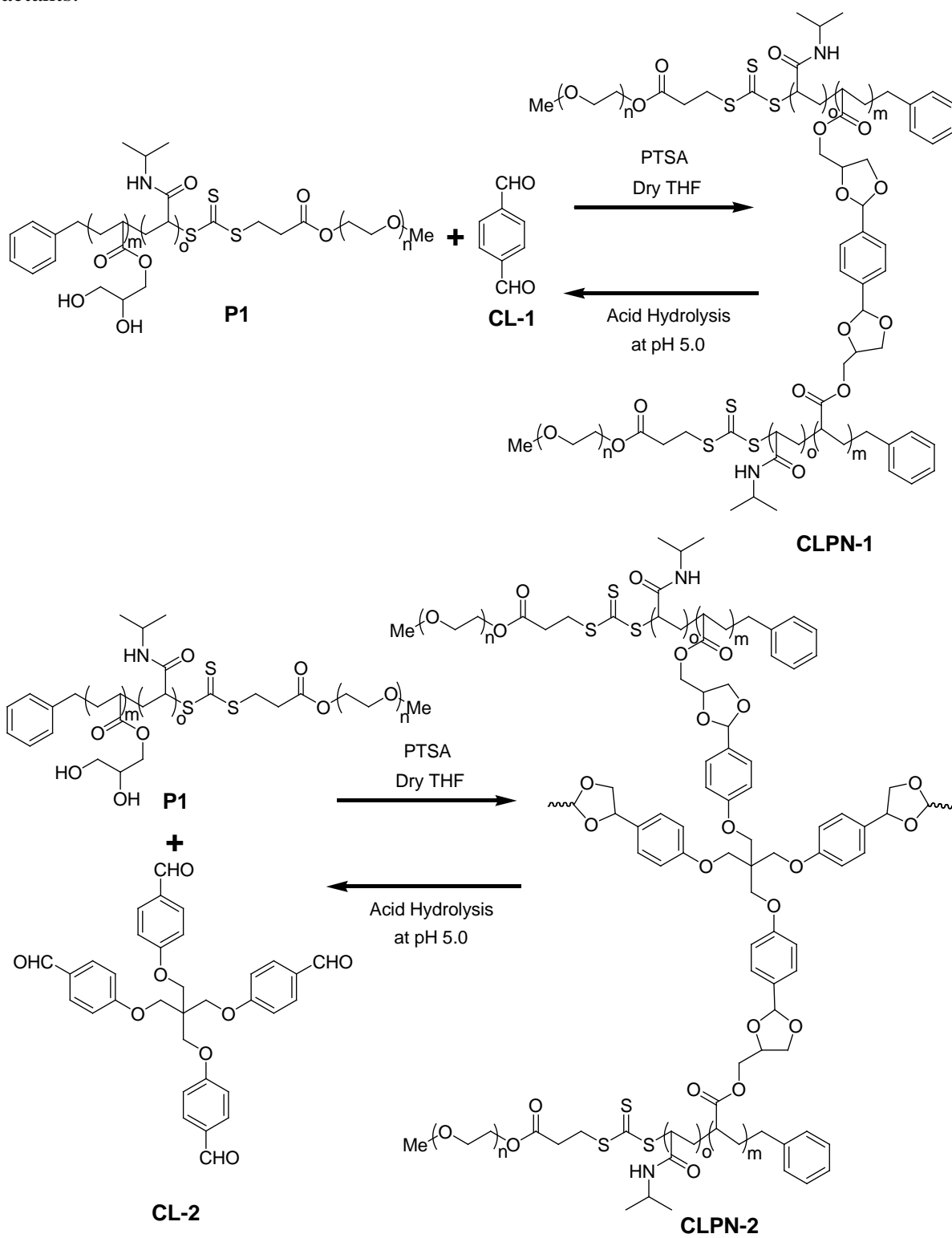
EXPERIMENTAL

Materials: Nile red and terephthalaldehyde (**CL-1**) were purchased from Sigma-Aldrich and used as received. All the other chemicals and solvents were purchased from SRL and Spectrochem (India) and purified by standard procedures. All cell culture media and fetal bovine serum (GIBCO, Invitrogen Corp, CA, USA), doxorubicin hydrochloride (DOX.HCl) (Sigma-Aldrich), propidium iodide (PI) (Sigma-Aldrich), 4′,6-diamidino-2-phenylindole dihydrochloride (DAPI) (Sigma-Aldrich), and 3-(4, 5-dimethylthiazol-2-yl)-2, 5-diphenyltetrazolium bromide (MTT) (Sigma-Aldrich), ribonuclease A (Sigma-Aldrich), trypsin (Himedia, Mumbai, INDIA) were purchased from the respective companies. Stock solutions of PI, DAPI and MTT were prepared by dissolving 1 mg of each compound in 1 ml PBS. The solutions were protected from light, stored at 4 °C, and used within 1 month. Stock concentrations of 10 mg/ml RNase A were prepared and kept at 20 °C.

Synthesis of CLPNs via the formation of acetal: Details of the synthesis of the triblock copolymer poly(ethylene glycol)-*b*-poly(N-isopropylacrylamide)-*b*-poly(glycidyl methacrylate) followed by ring-opening of the epoxide groups which produced the desired diol functionalized block copolymer[39] (**P1**), as well as the synthesis of the tetra-arm aldehyde cross-linker[40] (**CL-2**, Scheme 1) has been reported by us previously. The CLPNs were synthesized via acetal formation using the procedure as follows (see Scheme 1). In a 50 mL round bottomed flask, diol functionalized triblock copolymer, **P1,** (0.1 g, 0.21 mmol) was dissolved in 15-20 mL of dry

THF and mixed with the desired amount of **CL-1** or **CL-2** in presence of 3Å molecular sieves under argon atmosphere. The flask was then placed in a preheated oil bath at 70 °C and refluxed for 6-7 h in presence of catalytic amount of p-toluenesulfonic acid (PTSA). Thereafter, the reaction mixture was cooled and filtered and the filtrate slowly added to large excess of diethyl ether in order to recover the polymer as a precipitate. The process was repeated for three times and the final precipitate was washed thoroughly with ether, collected and dried under high vacuum for overnight to afford cross-linked polymer as a yellowish solid powder. The formation of core cross linked network was confirmed from GPC, ^{1}H NMR, and TEM images.

Methods: ^{1}H NMR spectra were obtained on a Bruker DPX-200 and 400 MHz NMR spectrometer, spectra were calibrated using residual solvent signal as the internal standard. Molecular weight and PDI of the polymers were determined by a GPC instrument (Viscotek) using RI detector and THF as eluent at a flow rate 1 ml/min. The molecular weights were calculated relative to polystyrene standards. The absorption and fluorescence spectra were collected using a Shimadzu (model no. UV-1601) UV-vis spectrophotometer and Hitachi (model no. F-7000) spectrofluorometer respectively. A negative staining technique was used for the transmission electron microscopy (TEM) studies. A drop of the sample solution was allowed to settle on a carbon coated copper grid for 1 min. Excess sample was wiped away with filter paper, and a drop of 1% uranyl acetate solution in methanol was allowed come in contact with the sample for 1 min. The samples were then air dried and analyzed using a JEOL JEM 100CX microscope operating at 80 kV. The hydrodynamic diameter (D_H) of the core cross-linked polymer nanoparticles were obtained from dynamic light scattering at variable temperature using a Malvern Nano ZS instruments equipped with a thermostatic sample chamber employing a 4 mW He-Ne laser operating at wavelength of 633 nm and a detector placed at 173°.

Scheme1. Schematic representation of the preparation of core cross-linked polymer nanoparticles (CLPNs) via acetal formation. Acid hydrolysis of the CLPNs gives back the reactants.

Encapsulation and release of Nile Red: For this experiment, **CLPN-1** (Scheme 1) was used as a representative CLPN. Nile Red (9.56 mg, 30 µmol, 30 eq per polymer chain) was mixed with 10 mg of the **CLPN-1** in 1 mL of HPLC grade DMSO, followed by addition to 20 mL of PBS buffer (pH-7.4) at the rate of approximately 10 µL/min under vigorous stirring. This solution was stirred at 20 °C for 16 h. Thereafter, the excess Nile Red and DMSO were completely removed by dialysis of the CLPN solution at 20 °C against a dialysis tubing of molecular cutoff 3 kD. The encapsulation was then confirmed by fluorescence spectroscopy (λ_{ex} = 550 nm). The release of Nile Red was monitored by fluorescence spectroscopy (λ_{ex} = 550 nm).

Doxorubicin (DOX) loading and in vitro release: For this experiment, **CLPN-2** (Scheme 1) was used as representative CLPN. Prior to use, a weighed amount of doxorubicin hydrochloride (DOX.HCl) was neutralized by stoichiometric amount of 10 mM sodium hydroxide solution in water. The neutralized DOX solution was then freeze-dried, redissolved in ethanol, and filtered through a 0.2 µm membrane filter to remove the precipitated salt. For loading of DOX in **CLPN-2**, **CLPN-2** (20 mg) and DOX (5 mg) were dissolved in 2 mL of DMSO, which was then added to 20 mL of an aqueous 0.1 M PBS buffer (pH 7.4) solution dropwise under vigorous stirring for 15 h at 40 °C to form a solution of drug-loaded **CLPN-2**. The solution was dialyzed against 500 mL of 0.1 M PBS buffer (pH 7.4) for 24 h at 40 °C through a membrane, MWCO 3 kDa. The buffer was replaced every 4 h to remove the unloaded free drug and DMSO. Thereafter, the amount of drug loaded in the **CLPN-2** solution was checked using UV absorbance at 480 nm. Loading of DOX was done at 20 °C following the same procedure. However as the loading of DOX was significantly higher at 40 °C, the release experiments were carried out with DOX loaded **CLPN-2** in which the loading was done at 40 °C. The drug loaded **CLPN-2** solution was divided into four equal portions, the first portion was dialyzed against 0.1 M PBS buffer

(pH=7.4) and the second portion was dialyzed against 0.1 M acetate buffer (pH=5.0) at 20 °C, and the remaining two portions were dialyzed against 0.1 M PBS buffer (pH=7.4) and 0.1 M acetate buffer (pH=5.0) at 37 °C. The aqueous medium outside the dialysis tube was withdrawn periodically to determine the drug concentration and the amount of the buffer was held constant by adding fresh buffer of same volume after each sampling. The amount of drug release was determined by UV-Vis spectroscopy.

Cell culture studies: Cervical cancer cell lines, HeLa and SiHa, were obtained from the National Center for Cell Science (NCCS), Pune, India and cultured. Cells were cultured in minimum essential media supplemented with 10% fetal bovine serum and incubated at 37 °C in a 5% CO_2 and 95% humidified incubator. Mycoplasma status of all cell lines has been detected through DAPI staining procedures.

Cell viability assay: MTT assay was performed to investigate the cell viability of the precursor polymer (**P1**) and the CLPNs on the growth of NIH/3T3 mouse fibroblast cells and that of **CLPN-2** on cervical cancer cells, HeLa and SiHa, in a dose dependent manner. Cells in logarithmic phase (1×10^4 cells/well) were seeded in 96-well tissue culture plates and allowed to grow for 16 h at 5% CO_2, 37 °C. Subsequently, the cells were treated with **P1** as well as the CLPNs at varying concentrations for 48 h. Cell viability was measured by MTT dye reduction assay at 540 nm with slight modifications in protocol reported by Younes et al. [41]

Cellular uptake studies: Uptake of DOX encapsulated CLPNs were analyzed using flow cytometry. Side scatter of the cells in flow cytometric analysis is a measure of complexity or granularity of the cells. As the drug loaded nanoparticles are taken in by the cells, the intensity of side-scattered light (SSC) of the cells increase.[42] A time dependent analysis of count vs SSC was

performed to quantify the cellular uptake of the nanoparticles by the cells. The results were further validated by fluorescent microscopy.

Cytotoxicity and induction of apoptosis: To investigate the time dependent effect of free DOX and DOX encapsulated CLPNs on the growth of HeLa and SiHa cells, MTT dye reduction assay was performed in the same procedure as described above. The time dependent curves of free DOX and DOX encapsulated nanoparticles were analyzed using Prism software (GraphPad Prism 5 software). Induction of apoptosis and associated morphological changes were studied by DAPI nuclear staining. HeLa and SiHa cells were seeded on coverslips in their selective complete medium respectively. After 24 h, the cells were treated with IC50 values of DOX encapsulated nanoparticles for 48 h. Cells were fixed in 3.7% paraformaldehyde, and permeabilized with 0.1 % Triton X-100 and then blocked in 2 % BSA, and stained with DAPI nuclear stain as per manufacturer's instructions. The cells were analyzed by confocal laser scanning microscopy (Olympus FluoView FV1000, Version 1.7.1.0) using the appropriate wavelength. The images were captured and digitized using FLUOVIEW 1000 (Version 1.2.4.0) imaging software. The results were further validated with flow cytometric cell cycle analysis. The cells were grown and treated with slightly lower dose than the IC50 value of DOX encapsulated CLPNs for 12, 24 and 48 h and with control treatment (0.1% DMSO) in cell culture dishes for 48 h. At the end of the treatment, the cells were washed with phosphate buffered saline (PBS) and fixed with 70% ethanol overnight at -20 °C. The next day, the cells were washed again with PBS and treated with RNase A (at a final concentration of 100 μg/ml) and propidium iodide (PI) incubation at a final concentration of 40 µg/ml, and the cells were incubated for 45 min. Finally, the cells were analyzed with the FACS Vantage SE (BD Corporation, Franklin Lakes, NJ, USA), and Cell Quest software version 2.0 (BD) was used for data analysis.

RESULTS AND DISCUSSIONS

Synthesis of CLPNs by acetal formation: Acetals possess some unique properties, that make them suitable for use in the preparation of acid-degradable drug delivery systems.[43-47] The acetal molecule consists of two single-bonded oxygen atoms attached to the same carbon atom which is formed reversibly in presence of catalytic amount of p-toluenesulfonic acid (PTSA) under dry condition via acid-catalyzed dehydration reaction of aldehyde and diols. In an acidic solution, one of the oxygen atoms of the acetal group is protonated, which activates the neighboring carbon. This facilitates the attack of water, resulting in the cleavage of the acetal to form the corresponding aldehyde and alcohol. In this work, we have aimed at establishing a simple synthetic approach for the synthesis of core cross-linked polymeric nanoparticles (CLPNs) through diol-aldehyde acetal formation between a diol functionalized triblock copolymer and two different aldehyde functionalized cross-linkers. The targeted CLPNs were synthesized using desired mole % of **CL-1** and **CL-2** with respect to the diol functionalities of the triblock copolymer, **P1** (Scheme 1), in presence of catalytic amount PTSA in dry THF for 6-7 h under refluxing conditions (Table 1). The formation of cross-linked polymers was confirmed from GPC, DLS and TEM analysis. GPC traces of the CLPNs revealed disappearance of the peak at ~17.58 mL corresponding to **P1** (M_n~23,500, PDI~1.35), and appearance of the major peaks at ~15.85 mL and ~15.1 mL for **CLPN-1** and **CLPN-2** respectively (Figure 1), indicating the presence of high molecular weight cross-linked polymer networks via formation of acetal linkages. Additional information about the cross-linking was obtained from ^{1}H NMR spectroscopy. The complete attenuation of the peak corresponding to the protons of GMA-diol units of **P1** at δ 3.95, δ 4.6 and δ 4.8, (refer Electronic Supplementary information of reference 37 for ^{1}H NMR spectra of **P1**) suggested that the core of the polymer networks were

significantly desolvated, further confirming the formation of the cross-linked networks. The

desolvated nature of the cross-linked networks is in agreement with the synthesized core cross-

Table 1: Feed composition and characterization of core cross-linked polymer nanoparticles (CLPNs, Scheme 1)

Sample code	Cross-linker used	Conc. of diol functional-ity from **P1**[a] (mmol)	Mol% of cross-linker (w.r.t diol)	Mn^b	PDI	Approx. no. of block copolymer chains per CLPN	Hydrodynamic diameter in water at 20 °C (at 37 °C) (nm)[c]
CLPN-1	**CL-1**	0.21	25.0	267,600	1.48	12	93 (123)
CLPN-2	**CL-2**	0.21	12.5	341,000	1.40	16	112 (139)

[a]Mn and PDI of **P1**, as measured by GPC, was ~23,500 and 1.35 respectively; [b]from GPC and [c]from DLS
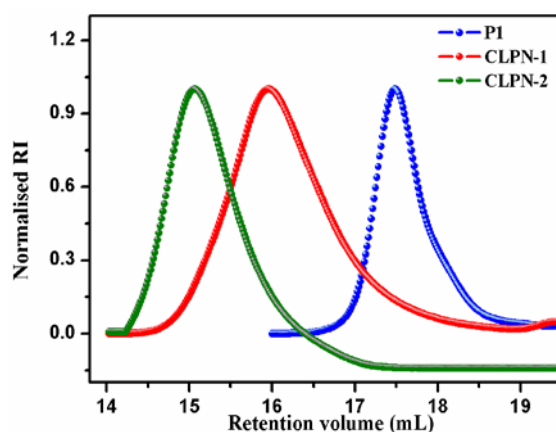

Figure 1. GPC traces of the core cross-linked polymer (**CLPN-1**, red and **CLPN-2**, olive) along with the diol functionalized triblock copolymers (**P1**, blue).
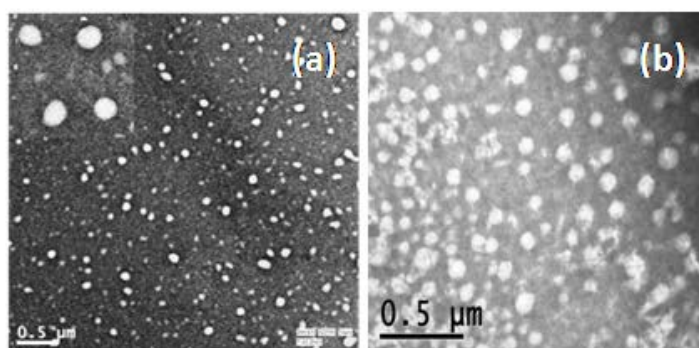

Figure 2. TEM images of aqueous solution of CLPNs: (a) **CLPN-1** (0.5 mg/mL), inset shows image with higher magnification; (b) (**CLPN-2**, 0.5 mg/mL) at 20 °C respectively.

linked polymers reported by Sumerlin et al.[23] and Fulton et al.[25] Figure 2 shows the TEM images

of the two CLPNs. The sizes were observed to be in the range of 80-110 nm for both the water-

soluble CLPNs. The images also indicated the spherical nature of the cross-linked nanoparticles

in aqueous solution. The sizes of the CLPNs were further determined from DLS experiments, the

average hydrodynamic size of the core cross-linked polymers in water at 20 °C was 93 nm and

112 nm for **CLPN-1** and **CLPN-2** respectively whereas for the hydrodynamic size of **P1** was ~ 8

nm. This large increase in the hydrodynamic size along with TEM images confirmed formation

of CLPNs.

The pH-triggered degradation of the core and as a result, disassembly of the CLPNs was

confirmed from DLS, Nile Red fluorescence spectroscopy and the release profile of the drug,

DOX. The CLPNs formed through acetal linkage expected to dissociate at low pH (pH~ 5.0),

resulting in the formation of the same linear polymer (**P1**) and the cross-linkers in solution. The

change of hydrodynamic size from 93 nm (for **CLPN-1)** and 112 nm (for **CLPN-2)** to ~10 nm at

pH~5.0 after incubation for 48 h indicated a nearly complete breakage of the nanoparticle

structures as a result of acid catalyzed cleavage of acetal bonds. The pH-triggered disassembly of

the CLPNs resulted in the formation of their component unimolecular polymer chains, which

was further confirmed using Nile Red as fluorescent probe. It is known that Nile Red as such has

poor solubility in water due to which an aqueous solution of Nile Red shows very weak

fluorescence with emission maxima at 661 nm (λ_{ex} = 550 nm). But, the emission intensity of Nile

Red increases dramatically on encapsulation in a hydrophobic domain.[48-49] In the present work,

Nile Red was encapsulated in **CLPN-1** at 20 °C in phosphate buffer of pH=7.4. Following this,

the pH of the solution was adjusted to 5.0 to trigger the disassembly of the core and as a

consequence, the release of the hydrophobic dye molecules. The noticeably less intense color of

the solution along with the gradual decrease of emission intensity of Nile Red suggested the

release of the dye molecules to the aqueous medium as the CLPNs disassembled to their unimolecular polymer chains in solution (Figure 3). For further study of the acid catalyzed degradation process, drug (DOX) loading and release studies were done with **CLPN-2**.
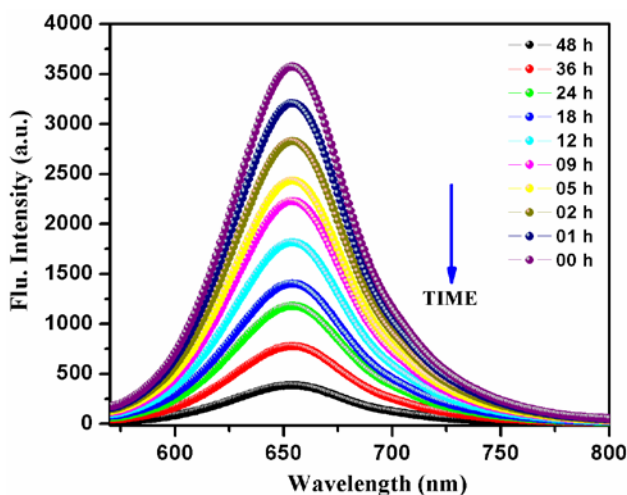

Figure 3. Nile Red emission spectra, which shows the release property of hydrophobic dye from the **CLPN-1** in mild acidic solution (pH~5) of different time interval at 20 °C temperature.

*pH and Temperature Triggered Drug Release Study from **CLPN-2***: In addition to Nile Red, we have considered DOX as a model hydrophobic drug for the loading and release experiments. The loading capacity (LC) and release (%; at time t) of DOX were calculated based on the following equations:

LC = [(Total amount of drug loaded)/(amount of the CLPN)] × 100 %

Release (%; at time t) = [(mass of drug released at t)/(total mass of drug encapsulated)] × 100 %

The LC of the cross-linked nanoparticles were determined by measuring the UV-Vis absorbance of DOX at 480 nm and fitted against a calibration curve. The loading capacity (LC) was determined at two different temperatures at pH~7.4. LC values were found to be 29.6 % and 20.8 % at 40 °C and 20 °C respectively for **CLPN-2**. From the above LC data, it may be noted that the loading of the hydrophobic drug DOX was considerably higher at higher temperature (40 °C)

than at lower temperature (20 °C). The hydrophobic domains formed by the PNIPA chains above its LCST led to higher encapsulation of the hydrophobic drug. LC data also suggested that when the loading was carried out at 40 °C, ~30% of the total amount of encapsulated DOX was by the PNIPA hydrophobic domains and ~70% of the total amount of encapsulated drug was loaded in the hydrophobic core of **CLPN-2**. DOX loaded **CLPN-2** in which the loading was done at 40 °C was further used for drug release study *in vitro*. The drug release profile from **CLPN-2** was evaluated at two different pH (5.0 and 7.4) as well as two different temperature (37 °C and 20 °C), and the data are presented in Figure 4. The following observations can be made from the drug release profiles – (i) at 20 °C, there was a sudden release of a fraction of the loaded drug within the first hour followed by a slow release of the encapsulated drug, (ii) at 37 °C, the release of drug was slow and gradual and final released amount was less compared to 20 °C, (iii) highest amount of drug release happened at pH~5.0 and 20 °C whereas the lowest occurred at pH~7.4 and 37 °C. As discussed earlier, when the DOX loading was done at 40 ºC, the majority of the hydrophobic drugs got encapsulated in the hydrophobic cross-linked core and a minor amount got loaded in the hydrophobic domains formed by the PNIPA chains. Hence, when the release experiments were carried out at 20 ºC, the PNIPA chains became hydrophilic and the drugs that were entrapped in the PNIPA domains were released immediately. The acid catalyzed degradation of the core took place at a comparatively much slower rate, enabling controlled release of the drug from the cross-linked core. The rate of hydrolysis of the acetal moiety of **CLPN-2** under mild acidic condition resulted in a significantly controlled release of the entrapped hydrophobic guest molecules. More than 80% of the loaded drug molecules were freed from the acetal functionalized cross-linked networks after incubation for approx. 20 h in an acidic environment (pH~ 5.0) at 20 °C.
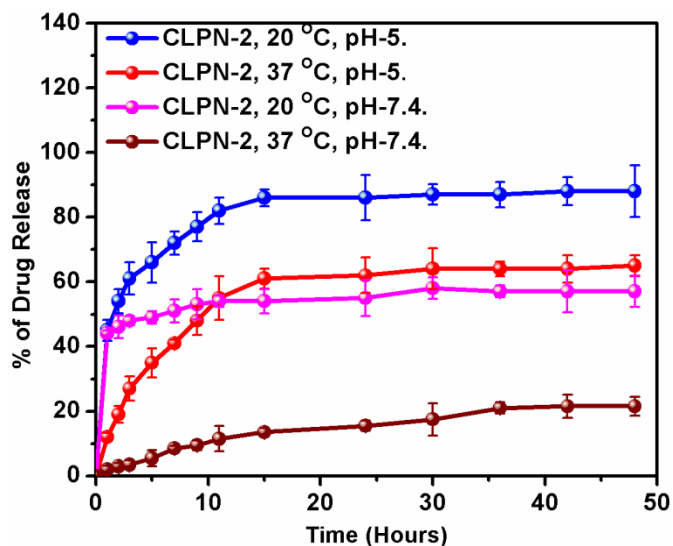
Figure 4: Release profile of model drug DOX with time from temperature and pH responsive cross-linked polymer (**CLPN-2**). Error bars represent ± (standard deviation) of three measurements.

*Biological study of DOX loaded **CLPN-2**:* In order to assess the safety of the CLPNs for drug delivery applications, the viability of normal cells in presence of the CLPNs and **P1** was studied up to 200 μg/ml by MTT dye reduction assay on normal mouse fibroblast cells, NIH/3T3. The results are shown in Figure 5a. Since the CLPNs were found to be non-toxic even at this high concentration, we went ahead to evaluate their capability to deliver drugs to the cancer cells. These experiments gave us the IC50 values of the DOX-loaded **CLPN-2** (discussed later). To check the toxicity of the **CLPN-2** without DOX to cancer cells, the cell viability of **CLPN-2** was also checked on HeLa and SiHa cells upto 80 µg/ml, which is significantly higher than the concentration of **CLPN-2** corresponding to the IC50 value of DOX-loaded **CLPN-2**. The data are presented in Figure 5b which shows that the **CLPN-2** was nontoxic to the two cancer cells evaluated.

HeLa and SiHa cell lines were further treated with varying concentrations of free (0 µM - 25 µM) and **CLPN-2** encapsulated DOX (0 µM - 50 µM) for 48 h. MTT dye reduction revealed that the IC50 for the nanoparticle encapsulated DOX was reduced to 1.592 ± 0.92 µM and 2.147 ±

0.98 µM as compared to 3.68 ± 0.95 µM and 7.552 ± 0.96 µM for free DOX, in HeLa and SiHa

cell lines respectively (Figure 6). This indicates that **CLPN-2** increased the extent of drug uptake

into the cervical cancer cell lines, HeLa and SiHa, by decreasing the loss of DOX before
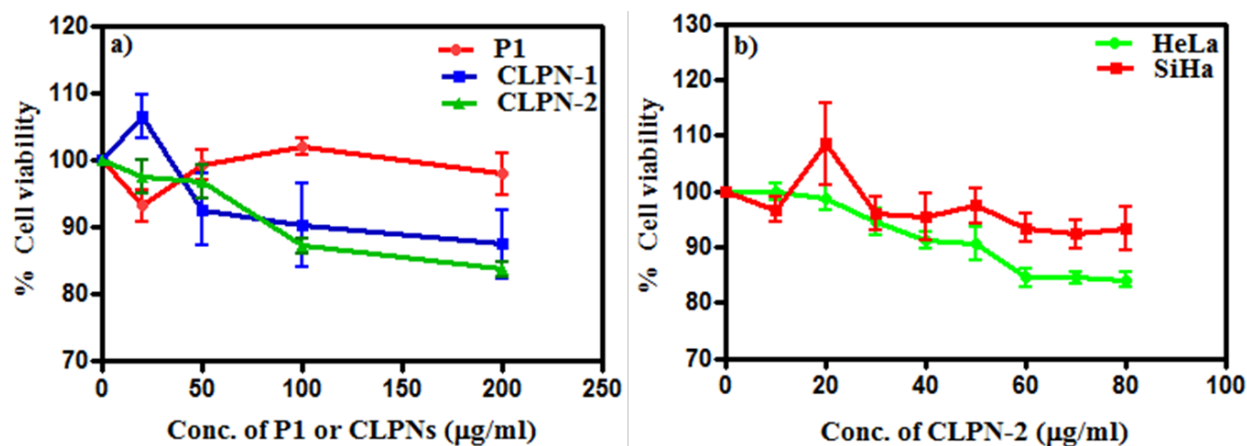
reaching the target site.

Figure 5: Cell viability assay of a) **P1**, **CLPN-1** and **CLPN-2** conducted on normal cell line, NIH/3T3; b) CLPN-2 on cervical cancer cell lines HeLa and SiHa. Error bars represent ± (standard deviation) of three measurements.
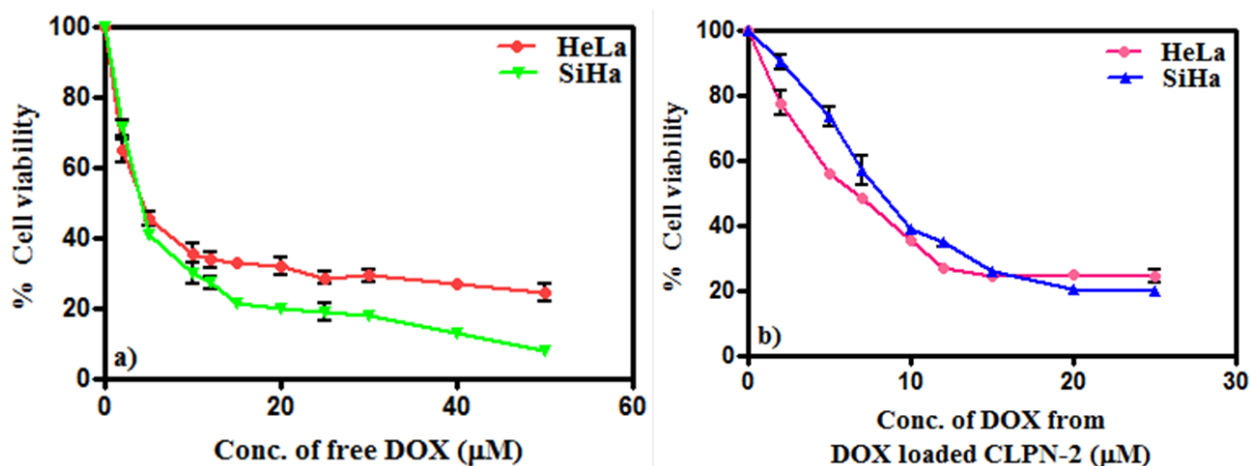

Figure 6. Cell viability assay of a) free DOX and b) DOX encapsulated **CLPN-2** against HeLa and SiHa cervical cancer cell lines. Error bars represent ± (standard deviation) of three measurements.

The cellular uptake of DOX encapsulated CLPNs was studied qualitatively by fluorescence imaging and quantitatively by flow cytometric analysis in cervical cancer cell lines in a time-dependent manner. Using flow cytometer, the amount of particles incorporated into the cells could be quantitatively characterized by the intensity of the side scattered light (SSC). There was a marked increase in the intensity of SSC with increasing period of incubation, indicating a time dependent uptake of the encapsulated drug (Figure 7). On treating the cells with **CLPN-2** encapsulated DOX for specified time period and observing them microscopically after washing with PBS, a better time-dependent internalization and nuclear accumulation of doxorubicin via CLPN encapsulation, in comparison to free DOX was observed in both the cell lines due to passive cellular uptake, authenticated by the fluorescent micrographs (Figure 8). Reduction in IC50 dose on CLPN encapsulation observed in cell viability assays and also be attributed to better cellular uptake and enhanced nuclear accumulation. The induction of apoptosis by DOX encapsulated nanoparticles was studied by observing the morphological changes associated with apoptosis. Nuclear fragmentation, a characteristic feature of apoptotic cell death, was clearly
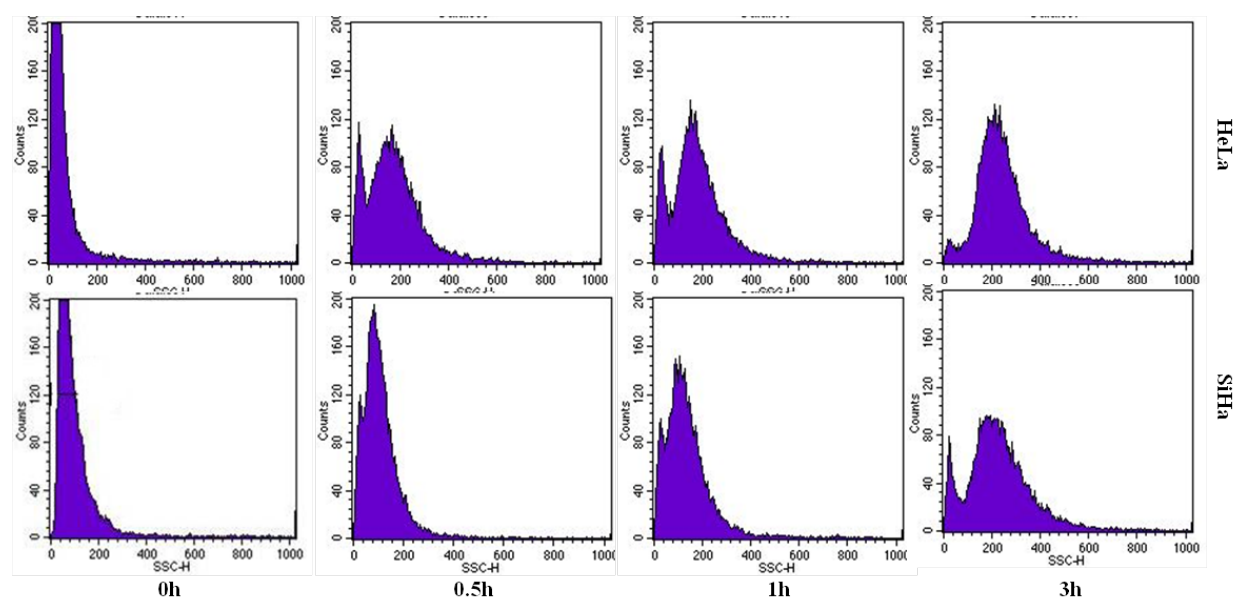

Figure 7. Cellular uptake by flow cytometry of DOX encapsulated **CLPN-2** into a) HeLa (top row) b) SiHa (bottom row) cells at different time periods; left to right: 0 h, 0.5 h, 1 h and 3 h.
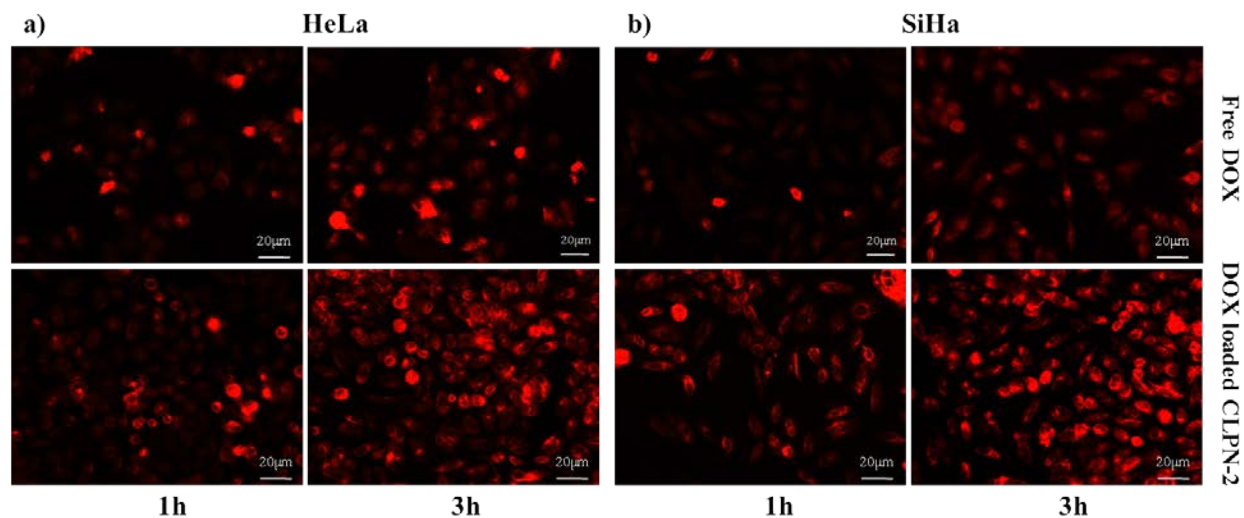
Figure 8. Fluorescent microscope images of free DOX and DOX loaded **CLPN-2** for 1 h (1st column) and 3 h (2nd column) - a) HeLa cells and b) SiHa cells. The length of the scale bars is 20 µm.
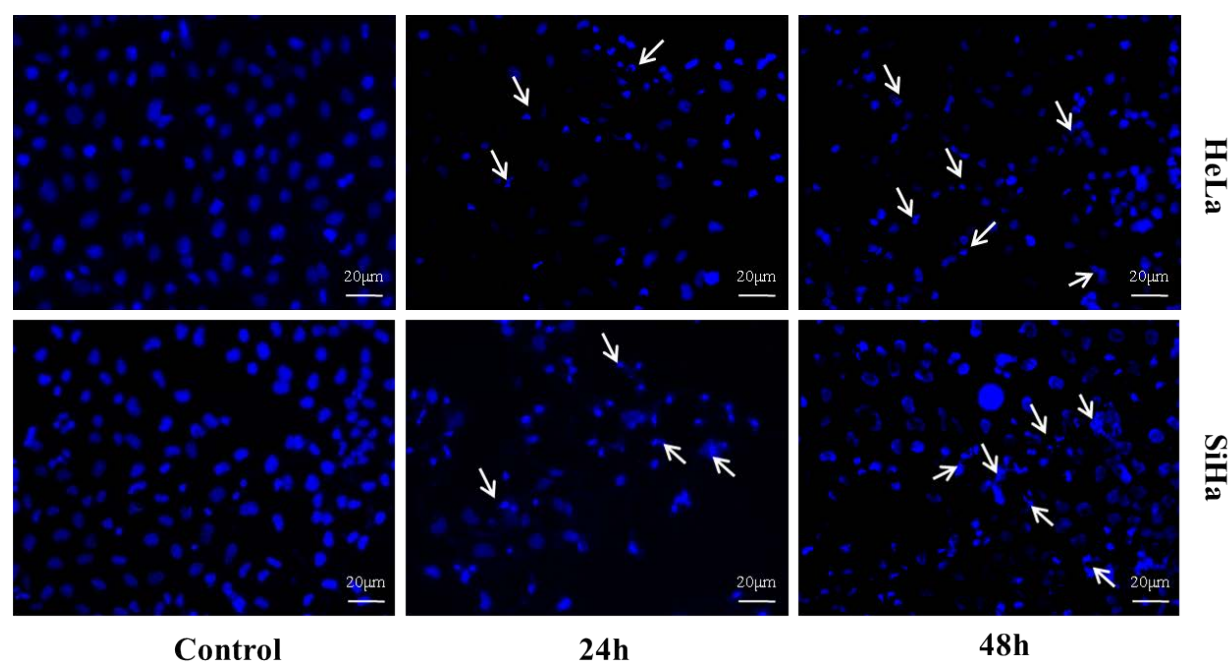

Figure 9. Induction of apoptosis by DOX encapsulated CLPNs was studied by observing characteristic morphological changes with the help of DAPI nuclear staining. Fluorescent microscope images of DAPI stained HeLa (top row) and SiHa cells (bottom row) after 24 h (middle column) and 48 h (right column) of treatment with DOX encapsulated **CLPN-2** along with the control (left column). The length of the scale bars is 20 µm.

demonstrated by DAPI staining (Figure 9). An increase in condensed and fragmented nuclei (shown by arrow in the figure) with increase in duration of treatment, indicated a time-dependent apoptotic cell death. It has been reported that DOX binds to DNA by intercalation and stimulates a series of biochemical events that ultimately leads to double-strand breaks and cell death via apoptosis.[50] In this regard, it can be stated that **CLPN-2** could efficiently release DOX to the tumor cells, thus preventing the proliferation of HeLa and SiHa cells effectively.
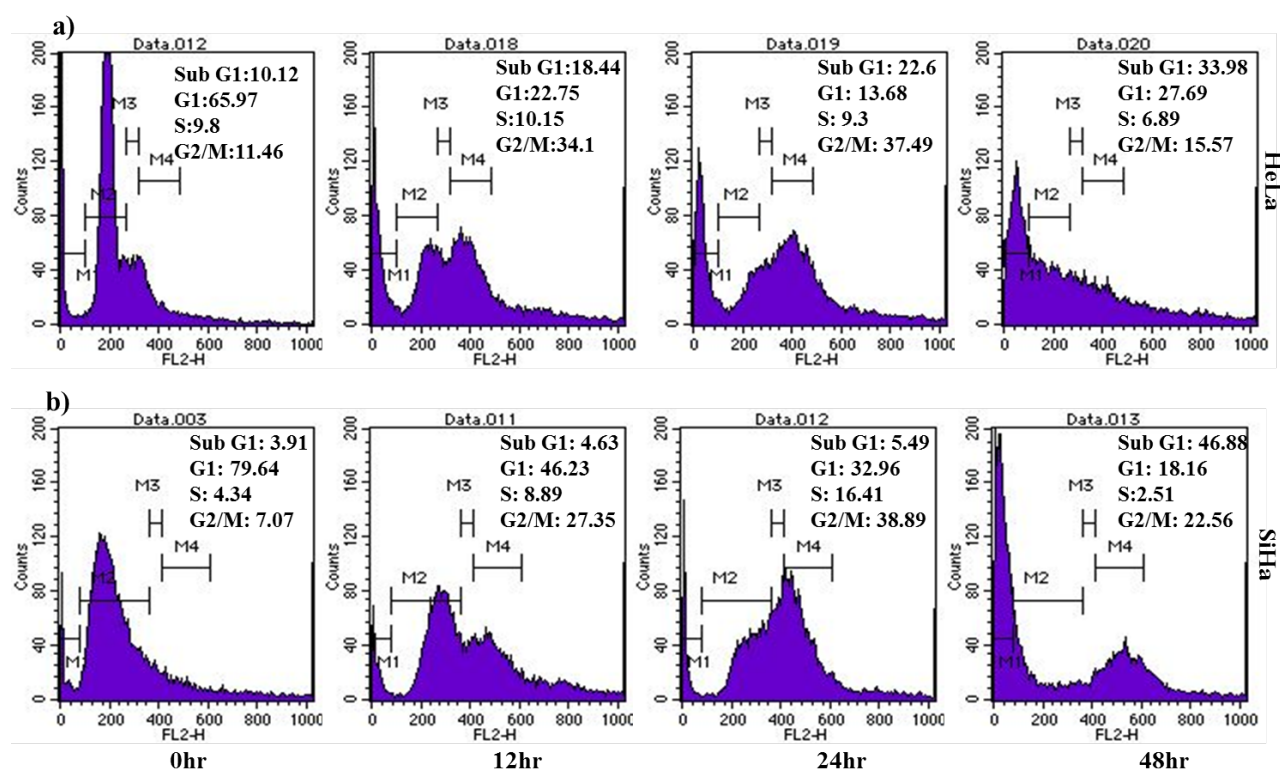

Figure 10. Cell cycle analysis was performed by treating cells with a slightly lower dose of IC50 value of DOX encapsulated **CLPN-2** at different time periods. Top row – HeLa, bottom row – SiHa cells. Left to right: 0 h, 12 h, 24 h and 48 h.

Apoptosis induction was further confirmed by cell cycle analysis. DOX is known to induce cell death by arresting the cell cycle at G2/M phase and by inducing DNA breakage. On treating HeLa and SiHa cells with **CLPN-2** encapsulated DOX with a dose slightly lower than the IC50, an initial arrest of the cell cycle in G2/M phase was observed till 24 h. However, after 48 h, sub

G1 population of cell cycle was found to be as high as 33.94% and 46.44% for HeLa and SiHa respectively (Figure 10) which is characteristic of DOX. It can therefore be concluded that, with encapsulation in **CLPN-2**, the antitumor efficacy of DOX can be achieved with a much lower dose compared to free DOX.

CONCLUSIONS

We have demonstrated a simple, versatile and efficient strategy to synthesize pH- and temperature responsive water-soluble core cross-linked polymer nanoparticles (CLPNs) by arm-first method via the formation of acetal linkage. Successively, their capability of loading and releasing of hydrophobic drug and dye molecules were studied. The CLPNs showed efficient loading of doxorubicin and the DOX-loaded CLPNs showed pH and temperature-dependent release of the encapsulated drug molecules, with the most favourable condition for delivery being lower temperature and desired lysosomal pH (~5.0) of the cancer cells. Non-toxicity of the CLPNs to normal mouse fibroblast cells, enhanced accumulation of the drug around the nucleus when treated with DOX-loaded CLPN as compared to free DOX as well as a significant reduction in IC50 of DOX-loaded CLPNs for HeLa and SiHa cells demonstrate great potential of these CLPNs for controlled drug delivery of anticancer drugs.

REFERENCES

(1) Xiaoa, K.; Luoa, J.; Lia, Y.; Leea, J. S.; Funga, G.; Lama, K. S. PEG-Oligocholic Acid Telodendrimer Micelles for the Targeted Delivery of Doxorubicin to B-Cell Lymphoma. *J. Control Release* **2011**, *155*, 272-281.

(2) Monsuez, J. J.; Charniot, J. C.; Vignat, N.; Artigou, J. Y. Cardiac Side-Effects of Cancer Chemotherapy. *International Journal of Cardiology* **2010**, *144*, 3-15.

(3) Chen, J.; Liu, Q.; Xiao, J.; Du J. EpCAM-Antibody-Labeled Noncytotoxic Polymer Vesicles for Cancer Stem Cells-Targeted Delivery of Anticancer Drug and siRNA. *Biomacromolecules* **2015**, *16*, 1695-1705.

(4) Joralemon, M. J.; McRae, S.; Emrick, T. PEGylated Polymers for Medicine: From Conjugation to Self-Assembled Systems. *Chem. Commun.* **2010**, *46*, 1377-1393.

(5) Wena, Y.; Oh, J. K. Dual-Stimuli Reduction and Acidic pH-Responsive Bionanogels: Intracellular Delivery Nanocarriers with Enhanced Release. *RSC Adv.* **2014**, *4*, 229-237.

 (6) Lv, J.; Sun, H.; Zou, Y.; Meng, F.; Dias, A. A.; Hendriks, M.; Feijen, J.; Zhong, Z. Reductively Degradable α-Amino Acid-Based Poly(Ester Amide)-Graft-Galactose Copolymers: Facile Synthesis, Self-Assembly, and Hepatoma-Targeting Doxorubicin Delivery. *Biomater. Sci.* **2015**, *3*, 1134-1146.

(7) Barenholz, Y. Doxil®-The First FDA-Approved Nano-Drug: Lessons Learned. *J. Controlled Release* **2012**, *160*, 117-134.

(8) Sahoo, B.; Devi, K. S. P.; Banerjee, R.; Maiti, T. K.; Pramanik, P.; Dhara, D. Thermal and pH Responsive Polymer-Tethered Multifunctional Magnetic Nanoparticles for Targeted Delivery of Anticancer Drug. *ACS Appl. Mater. Interfaces* **2013**, *5*, 3884-3893.

(9) Jackson, A. W.; Fulton, D. A. Making Polymeric Nanoparticles Stimuli-Responsive with Dynamic Covalent Bonds. *Polym. Chem.* **2013**, *4*, 31-45.

(10) Jackson, A. W.; Stakes, C.; Fulton, D. A. The Formation of Core Cross-Linked Star Polymer and Nanogel Assemblies Facilitated by The Formation of Dynamic Covalent Imine Bonds. *Polym. Chem.* **2011**, *2*, 2500-2511.

(11) Wanga, Z.; Chen, C.; Zhang, Q.; Gao, M.; Zhang, J.; Kong, D.; Zhao, Y. Tuning The Architecture of Polymeric Conjugate to Mediate Intracellular Delivery of Pleiotropic Curcumin. *Eur J Pharm Biopharm.* **2015**, *90*, 53–62.

(12) Yang, R.; Zhang, S.; Kong, D.; Gao, X.; Zhao, Y.; Wang, Z. Biodegradable Polymer-Curcumin Conjugate Micelles Enhance the Loading and Delivery of Low-Potency Curcumin. Pharm Res. **2012**, *29*, 3512-3525.

(13) Oyama, N.; Minami, H.; Kawano, D.; Miyazaki, M.; Maeda, T.; Toma, K.; Hottab, A.; Nagahama, K. A Nanocomposite Approach to Develop Biodegradable Thermogels Exhibiting Excellent Cell-Compatibility for Injectable Cell Delivery. *Biomater. Sci.* **2014**, *2*, 1057-1062.

(14) Kaur, S.; Prasad, C.; Balakrishnana, B.; Banerjee, R. Trigger Responsive Polymeric Nanocarriers for Cancer Therapy. *Biomater. Sci.* **2015**, *3*, 955-987.

 (15) Morinloto, N.; Qiu, X. P.; Winnik, F. M.; Akiyoshi, K. Dual Stimuli-Responsive Nanogels by Self-Assembly of Polysaccharides Lightly Grafted with Thiol-Terminated Poly(N-isopropylacrylamide) Chains. *Macromolecules* **2008**, *41*, 5985-5987.

(16) Tsarevsky, N. V.; Matyjaszewski, K. Combining Atom Transfer Radical Polymerization and Disulfide/Thiol Redox Chemistry: A Route to Well-Defined (Bio)degradable Polymeric Materials. *Macromolecules* **2005**, *38*, 3087-3092.

(17) Syrett, J. A.; Haddleton, D. M.; Whittaker, M. R.; Davis, T. P.; Boyer, C. Functional, Star Polymeric Molecular Carriers, Built From Biodegradable Microgel/Nanogel Cores. *Chem. Commun.* **2011**, *47*, 1449-1451.

(18) Thurmond, K. B.; Kowalewski, T.; Wooley, K. L. Water-Soluble Knedel-like Structures: The Preparation of Shell-Cross-Linked Small Particles. *J. Am. Chem. Soc.* **1996**, *118*, 7239-7240.

(19) Thurmond, K. B.; Kowalewski, T.; Wooley, K. L. Shell Cross-Linked Knedels: A Synthetic Study of the Factors Affecting the Dimensions and Properties of Amphiphilic Core-Shell Nanospheres. *J. Am. Chem. Soc.* **1997**, *119*, 6656-6665.

(20) Butun, V.; Lowe, A. B.; Billingham, N. C.; Armes, S. P. Synthesis of Zwitterionic Shell Cross-Linked Micelles. *J. Am. Chem. Soc.* **1999**, *121*, 4288-4289.

(21) Read, E. S.; Armes, S. P. Recent advances in shell cross-linked micelles. *Chem. Commun*. **2007**, 3021-3035.

(22) Li, Y.; Lokitz, B. S.; McCormick, C. L. Thermally Responsive Vesicles and Their Structural "Locking" through Polyelectrolyte Complex Formation. *Angew. Chem. Int. Ed.* **2006**, *45*, 5792-5795.

(23) Xu, X.; Flores, J. D.; McCormick, C. L. Reversible Imine Shell Cross-Linked Micelles from Aqueous RAFT-Synthesized Thermoresponsive Triblock Copolymers as Potential Nanocarriers for "pH-Triggered" Drug Release. *Macromolecules* **2011**, *44*, 1327-1334.

(24) Wiltshire, J. T.; Qiao, G. G. Synthesis of Core Cross-Linked Star Polymers with Adjustable Coronal Properties. *Macromolecules* **2008**, *41*, 623-631.

(25) Wiltshire, J. T.; Qiao, G. G. Selectively Degradable Core Cross-Linked Star Polymers. *Macromolecules* **2006**, *39*, 9018-9027.

(26) Bapat, A. P.; Roy, D.; Ray, J. G.; Savin, D. A.; Sumerlin, B. S. Dynamic-Covalent Macromolecular Stars with Boronic Ester Linkages. *J. Am. Chem. Soc.* **2011**, *133*, 19832-19838.

(27) Bapat, A. P.; Ray, J. G.; Savin, D. A.; Sumerlin, B. S. Redox-Responsive Dynamic-Covalent Assemblies: Stars and Miktoarm Stars. *Macromolecules*, **2013**, *46*, 2188-2198.

(28) Jackson, A. W.; Fulton, D. A. The Formation of Core Cross-Linked Star Polymers Containing Cores Cross-Linked by Dynamic Covalent Imine Bonds. *Chem. Commun.* **2010**, *46*, 6051-6053.

(29) Xu, X.; Smith, A. E.; Kirkland, S. E.; McCormick, C. L. Aqueous RAFT Synthesis of pH-Responsive Triblock Copolymer mPEO−PAPMA−PDPAEMA and Formation of Shell Cross-Linked Micelles. *Macromolecules* **2008**, *41*, 8429-8435.

(30) Jackson, A. W.; Fulton, D. A. Triggering Polymeric Nanoparticle Disassembly through the Simultaneous Application of Two Different Stimuli. *Macromolecules* **2012**, *45*, 2699-2708.

(31) Jackson, A. W.; Fulton, D. A. pH Triggered Self-Assembly of Core Cross-Linked Star Polymers Possessing Thermoresponsive Cores. *Chem. Commun.* **2011**, *47*, 6807-6809.

(32) Garbern , J. C.; Minami, E.; Stayton, P. S.; Murry, C. E. Delivery of Basic Fibroblast Growth Factor With A pH-Responsive, Injectable Hydrogel to Improve Angiogenesis in Infarcted Myocardium. *Biomaterials*, **2011**, *32*, 2407-2416.

(33) Klinger, D.; Landfester, K. Dual Stimuli-Responsive Poly(2-hydroxyethyl methacrylate-co-methacrylic acid) Microgels Based on Photo-Cleavable Cross-Linkers: pH-Dependent Swelling and Light-Induced Degradation. *Macromolecules* **2011**, *44*, 9758-9772.

(34) Chen, W.; Meng, F.; Li, F.; Ji, S. J.; Zhong, Z. pH-Responsive Biodegradable Micelles Based on Acid-Labile Polycarbonate Hydrophobe: Synthesis and Triggered Drug Release. *Biomacromolecules* **2009**, *10*, 1727-1735.

(35) Li, Y.; Armes, S. P. Synthesis and Chemical Degradation of Branched Vinyl Polymers Prepared via ATRP: Use of a Cleavable Disulfide-Based Branching Agent. *Macromolecules* **2005**, *38*, 8155-8162.

(36) Li, Y.; Lokitz, B. S.; Armes, S. P.; McCormick, C. L. Synthesis of Reversible Shell Cross-Linked Micelles for Controlled Release of Bioactive Agents. *Macromolecules* **2006**, *39*, 2726-2728.

(37) Bae, Y.; Fukushima, S.; Harada, A.; Kataoka, K. Design of Environment-Sensitive Supramolecular Assemblies for Intracellular Drug Delivery: Polymeric Micelles that are Responsive to Intracellular pH Change. *Angew. Chem. Int. Ed.* **2003**, *42*, 4640-4643.

(38) Liu, S.; Weaver, J. V. M.; Tang, Y.; Billingham, N. C.; Armes, S. P. Synthesis of Shell Cross-Linked Micelles with pH-Responsive Cores Using ABC Triblock Copolymers. *Macromolecules* **2002**, *35*, 6121-6131.

(39) Banerjee, R.; Dhara, D. Functional Group-Dependent Self-Assembled Nanostructures from Thermo-Responsive Triblock Copolymers. *Langmuir* **2014**, *30*, 4137-4146.

(40) Banerjee, R.; Maiti, S.; Dhara, D. Synthesis of Soluble Core Cross-Linked Polystyrene Star Polymer by Application of Acrylate-Nitrile oxide 'Click Chemistry' using Metal-Free Reagents. *Green Chem.* **2014**, *16*, 1365-1373.

(41) Younes, M. N.; Yigitbasi, O. G.; Park, Y. W.; Kim, S. J,; Jasser, S. A.; Hawthorne, V. S.; Yazici, Y. D.; Mandal, M.; Bekele, B. N.; Bucana, C. D.; Fidler, I. J.; Myers J. N. Antivascular Therapy of Human Follicular Thyroid Cancer Experimental Bone Metastasis by Blockade of Epidermal Growth Factor Receptor and Vascular Growth Factor Receptor Phosphorylation. *Cancer Res*. **2005**, *65*, 4716-4727.

(42) Lai, T. Y.; Lee, W. C. Killing of Cancer Cell Line by Photoexcitation of Folic Acid-Modified Titanium Dioxide Nanoparticles. *Journal of Photochemistry and Photobiology A: Chemistry* **2009**, *204*, 148-153.

(43) Murthy, N.; Thng, Y. X.; Schuck, S.; Xu, M. C.; Frechet, J. M. J. A Novel Strategy for Encapsulation and Release of Proteins: Hydrogels and Microgels with Acid-Labile Acetal Cross-Linkers. *J. Am. Chem. Soc.* **2002**, *124*, 12398-12399.

(44) Murthy, N.; Xu, M.; Schuck, S.; Kunisawa, J.; Shastri, N.; Fre´chet, J. M. J. A Macromolecular Delivery Vehicle for Protein-Based Vaccines: Acid-Degradable Protein-Loaded Microgels. *Proc. Natl. Acad. Sci. U. S. A.* **2003**, *100*, 4995-5000.

(45) Binauld, S.; Stenzel, M. H. Acid-Degradable Polymers for Drug Delivery: a Decade of Innovation. *Chem. Commun*. **2013**, *49*, 2082-2102.

(46) Goh, S. L.; Murthy, N.; Xu, M. C.; Frechet, J. M. Cross-Linked Microparticles as Carriers for the Delivery of Plasmid DNA for Vaccine Development. *Bioconjugate Chem.* **2004**, *15*, 467-474.

(47) Bulmus, V.; Chan, Y.; Nguyen, Q.; Tran, H. L. Synthesis and Characterization of Degradable p(HEMA) Microgels: Use of Acid-Labile Cross-linkers. *Macromol. Biosci.* **2007**, *7*, 446-455.

(48) Maiti, C.; Dey, D.; Mandal, S.; Dhara, D. Thermoregulated Formation and Disintegration of Cationic Block Copolymer Vesicles: Fluorescence Resonance Energy Transfer Study. *J. Phys. Chem. B* **2014**, *118*, 2274-2283.

(49) Maiti, C.; Banerjee, R.; Maiti, S.; Dhara, D. pH-Induced Vesicle-to-Micelle Transition in Amphiphilic Diblock Copolymer: Investigation by Energy Transfer between in Situ Formed Polymer Embedded Gold Nanoparticles and Fluorescent Dye. *Langmuir* **2015**, *31*, 32-41.

(50) Wang, H.; Zhao, Y.; Wu, Y.; Hu, Y. L.; Nan, K.; Nie, G.; Chen, H. Enhanced Anti-Tumor Efficacy by Co-Delivery of Doxorubicin and Paclitaxel with Amphiphilic Methoxy PEG-PLGA Copolymer Nanoparticles. *Biomaterials* **2011**, *32*, 8281-8290.